Defence Science Journal, Vol. 72, No. 4, July 2022, pp. 533-542, DOI : 10.14429/dsj.72.18001

Prediction of Initial and Striking Velocity of Primary Fragments from Cased Spherical Explosive inside Steel Cubical Structure

Prahalad Srinivas Joshi* and S.K. Panigrahi

Department of Mechanical Engineering, DIAT, Girinagar, Pune – 411 025, India
**Email:* prahjo20904@gmail.com

ABSTRACT

Usually, energy generated from an explosive's detonation is transferred partly in the form of the blast impulse and some in the form of the kinetic energy of casing fragments. When detonation occurs in an explosive casing, it breaks the casing into fragments of different weights with varying velocities. The extent of destruction by these energized fragments depends upon the initial velocity they gain after an explosion. The momentum gained by the fragments decides the capability to perforate a barrier or propagate an explosion. A three-dimensional non-linear FEA method is used to model a box-shaped steel structure. This box-shaped structure is subjected to an internal cased explosion for estimating the initial and striking velocities of primary fragments. The effect of varying charge weight and the effect of the sacrificial wall on the initial and striking velocity of fragments via numerical simulations are also carried out. The initial and striking velocity values obtained through simulation are compared with the design guidelines of the code-based approach, and a good agreement is reported.

Keywords: Explosive casing; Gurney equation; Initial velocity; Primary fragments; Striking velocity

1. INTRODUCTION

Usually, the high explosives (HE) are enclosed in metal casings while in service. Upon detonation, HE produces exceptionally high pressure and hot gasses, which in turn pressurizes the damaged inner walls of the metal casing to form primary fragments. When they impact surrounding structures, these primary fragments develop secondary fragments and influence the design of the armament and other protective structures. Thus, studying the fragment velocity could benefit design guidelines for the effectiveness of weapons consisting of HE in a closed container like a warhead or bomb.

A mathematical model was developed by assuming an infinitely long cylindrical casing, allowing only the radial motion of fragments and nullifying the effect of detonation in the longitudinal direction.[1] Based on this, initial velocities of fragments due to the detonation of metal casings filled with HE was calculated using Eqn. (1) and verified with experimental results.[2] The initial velocity of fragments is determined by the equation given below:

$$v_0 = \sqrt{2E}\sqrt{\frac{\beta}{1+0.5\beta}} \tag{1}$$

where v_0 is the initial velocity of fragments, $\sqrt{2E}$ is Gurney energy, E is contribution to the explosion's kinetic energy due to HE's unit mass, and β is the ratio of casing mass to explosive mass. Relation between stress state and thermo-plasticity of cylindrical metal casings filled with HE with a slight modification of Taylors[1] hypothesis of radial fracture mode was proposed by Hoggatt and Recht.[3] It has been observed that the walls of the metal casing accelerated radially outward due to compressive hoop stress produced during the detonation of the HE. It was also attempted to find speeds of metal layers after detonation in the case of multi-layered warheads by Jones.[4]

Jones-Wilkins-Lee equation[5-7] is widely used to study the reaction processes of detonation of HE. Gas leakage in an internal blast event was identified, and the Gurney equation was modified by multiplying by a factor of 0.8 to overcome. The factor accounted for the effect of gas leakage, which was verified by experimental results obtained by Charron.[8] The material properties of the metal casings and HE characteristics primarily affect the detonation outcome. Pearson[9] observed that the behavior of fragments is not a separate event and can influence the total system. A series of aluminium and copper cylinder expansion tests were carried out for a varied mass of explosive to mass of cylinder ratio and explosives. These were further verified by performing the expansion tests for evaluating and describing the acceleration characteristics of the metal fragments by Bola, *et al*. and Kury, *et al.*[10-11] Subsequently, many researchers[12-14] calculated the fragment velocities by modifying Gurney energy as mentioned in Eqn. (2), given below.

$$\sqrt{2E_G} = \frac{D}{3.08} \tag{2}$$

where, D is detonation velocity, and E_G is Gurney energy.

Received : 25 March 2022, Revised : 02 July 2022
Accepted : 15 July 2022, Online published : 26 August 2022

Maximum fragment velocity was calculated by considering the influence of the metal casing on the intensity of detonation. It was observed that not all parts of the metal casing could produce fragments. Thus, the total mass of the casing should not be considered while calculating the kinetic energy (E_G).[15] Furthermore, the polytropic coefficient was considered for modification of the Gurney equation, as mentioned in Eqn. (3)

$$E_G = \frac{D^2}{2\left(\Upsilon^2 - 1\right)} \quad (3)$$

where, E_G is the Gurney energy, D is detonation velocity, and Υ is the polytropic coefficient (usually taken as 3 for detonation products). It was reported that the subsequent fragment velocity computation turned out inaccurate.[16] The Gurney velocity was modified by considering the momentum of explosive gases and allowing the casing to fracture before fully expanding. However, dynamic testing of the metal casing would be required to establish the effect of explosion over the yield stress on the metal casings.[17]

A uniform expansion of the gas pressure was assumed in an attempt to establish a relation to find Gurney velocity

$$2E = \left(\frac{2M_1}{C} + \frac{1}{3}\right)V_1^2 + \left(\frac{M}{C} + \frac{1}{2}\right)G^2 \quad (4)$$

Here, E_G is the Gurney energy, V_1 is the velocity of fragments from end plates in the axial direction, M_1 is the mass of each end plate, M is the mass of cylindrical casing, C is the mass of explosive detonated, and G is Gurney velocity. Eqn. (4) is a modification of Eqn. (1), wherein the results found were in good agreement with Gurney's results.[18] Furthermore, an analytical approach was reported, with the objective of fast and reliable real-time simulation of the fragmentation process. Finally, a relation Eqn. (5) was presented to calculate primary fragment velocity based on Eqn. (4).

$$V = -G\frac{1-a}{\left(1-b\right)^2}\left(\frac{X}{L}\right)^2 + G \quad (5)$$

Here, V is initial fragment velocity, G is Gurney velocity, X is distance from point of detonation along height (L) of the cylindrical casing, $0 \le a \le 1$ where a is an experimental constant and $0.60 \le b \le 0.70$ which is also an experimental constant. However, it was cautioned about errors due to reduced pressure close to the end plates.[19]

A time-dependent, 2D finite-difference code program named HEMP, written in an expanded FORTRAN IV language, was used to mimic the fragmentation process.[20] The simulation showed unrealistically high deformations of the metal casings; thus, a separate gas leakage model was proposed. A model was created by Lindsay *et al.*[21] using information from a copper-cylinder expansion test. However, the model did not account for the casing and gas leakage disintegration. Hence, the acceleration of the fragments post-detonation was not accurate. Breech[22] assumed uniform expansion of the gas pressure to establish a relation to find Gurney velocity. The relation used was a modification of Eqn. (1), wherein the results were in good agreement with Gurney's results. A simulation model in AUTODYN was developed by Elek, *et al*.[23] based on the interaction of the detonation wave and metallic casing along with gas pressure in simultaneous events to study the acceleration of fragments of a cylinder with the axis-symmetric detonation of HE and validated with experimental results. The radial distribution of the fragment velocity was predicted by considering the velocity gains with an azimuth angle at 63 degrees in the target direction. The calculations were in close agreement with the experimental data of Wang, *et al*.[24] To investigate the fragmentation process of a cylindrical metal casing with HE, Xiangshao, *et al.*[25] used AUTODYN and Smoothed Particle Hydrodynamics (SPH) procedures. Validation with experimental findings confirmed that the path of the detonation wave is directly related to the expansion velocity of the casing.

Li, W *et al.*[26] studied the fragmentation effect by making external grooves on cylindrical metal casings at different depths. The results were used to develop a model in LS DYNA. Comparing simulation and experimental results, they reported that grooves and HE materials significantly affected fracture mechanisms. Grisrao and Dancygier[27] reported a good agreement for two-dimensional, three-dimensional, and SPH numerical models with experimental results for evaluating fragment velocities due to the explosion of cylindrical metal casings. It described the velocity of fragments using a normalized shape function that depended on the length to diameter ratio of the casing. Based on the Arbitrary Lagrangian-Eulerian formulation of the governing equations, a 2D and 3D axial symmetric high-rate finite-difference computer code called Picatinny Arsenal FRAGmentation (PAFRAG) was developed. The code could accurately predict fragmentation, verified with experimental data.[28]

Huang, *et al.*[29] investigated the initial velocity of fragments using an ash radiography technique and proposed a formula based on the Gurney equation. Later, Li. Y *et al.*[30] suggested a numerical model determine the influence of the incident angle of the detonation wave. Results confirm that the formula developed with a numerical model could accurately predict fragment speed dispersion along the axis and circumference of the cylindrical skin under an eccentric start point at one end, thereby simulating the edge effect. Further, Studies reported calculating the fragment velocity of hollow-core warheads with asymmetric detonation[31–34]. Recently, Jifeng Wei *et.al*[35] studied the fragmentation of a thin-walled Q235 steel shell under an explosion of TNT. They internally exploded two hollow cylindrical geometries with different length to diameter ratios with TNT of two different charge weights, and fragments were collected physically. They reported the mass and number of fragments and compared these experimental findings with two analytical formulae. The comparison was in good agreement.

From the above, it is inferred that the previous studies are primarily based on the estimation of fragment velocity through analytical methods and result validation by experimental method. In the case of fragmentation effect, both analytical and experimental methods suffer from inaccuracies due to the geometry involved, as end effects cannot be accounted for, and the measurement of fragment velocity close to the blast site is tedious. Hence, in the current work, the fragment velocities are predicted through simulation and validated through the UFC document's design code, eliminating these inaccuracies. The present work focuses on the fragmentation analysis of a spherical cased explosive inside a Q235 steel cubicle box under the internal blast of TNT through simulation. The box-shaped geometry is chosen for current work because of its generalized shape, representing a wide range of explosive containers like a large explosive storehouse or a simple Improvised Explosive Device (IED) container. Two different varying charge weights of TNT are considered for the explosion. First, the initial and striking velocities of primary fragments are estimated with United Facilities Criteria (UFC) based code approach[36] for both the charge weights. Then, simulation is carried out in LS DYNA to analyze the fragmentation process. Herein, Multi-Material Arbitrary Lagrangian-Eulerian (MMALE) method is adopted for high strain rate loading of the blast, where the Lagrangian domain is incorporated to model the cubical steel box structure, and the explosive is modeled in a Eulerian domain. The initial and striking velocities of primary fragments estimated through the UFC code approach are then compared with finite element-based numerical simulations. Further, the effect of the sacrificial wall on the initial and striking velocity of primary fragments via numerical simulations is also studied.

2. ESTIMATION OF INITIAL AND STRIKING VELOCITY OF PRIMARY FRAGMENTS WITH CODE BASED APPROACH

The initial velocities of primary fragments resulting from the detonation of metal casings of various shapes (Uniform and non-uniform cylindrical and spherical casings) filled with various types of HE is mentioned in Table 2.6 of chapter 2 of the UFC document.[36] In addition, the initial velocity of primary fragments resulting from the detonation of an evenly filled HE in a spherical casing, as shown in Fig. 1, is mentioned in Eqn. (6).

$$v_0 = \sqrt{2E\left[\frac{\frac{W}{W_C}}{1+\frac{3W}{5W_C}}\right]} \tag{6}$$

where, v_0 is initial velocity of fragments, $\sqrt{2E}$ is Gurney energy constant from Table 1, W is weight of explosive and W_C is weight of metal casing.

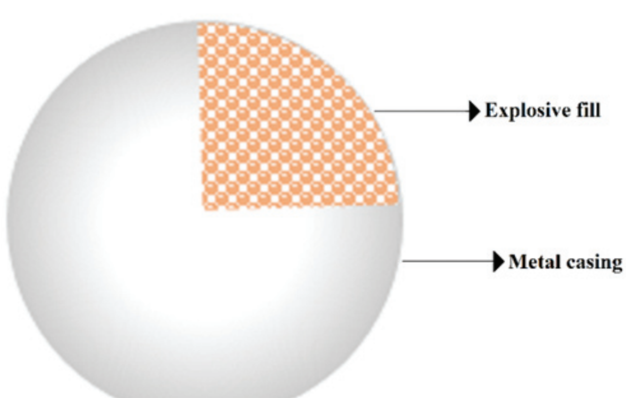

Figure 1. Schematic of spherical casing.

Table 1. Gurney energy constant for different explosives[36]

Explosive	$\sqrt{2E}$ (ft/sec)	$\sqrt{2E}$ (m/sec)
Composition B	9100	2773.68
Composition C-3 0.0578	8800	2682.24
HMX 0.0682	9750	2971.8
Nitromethane 0.0411	7900	2407.92
PBX-9404 0.0664	9500	2895.6
PETN 0.0635	9600	2926.08
RDX 0.0639	9600	2926.08
TACOT 0.0581	7000	2133.6
Tetryl 0.0585	8200	2499.36
TNT 0.0588	8000	2438.4
Trimonite No. 1	3400	1036.32
Tritonal (TNT/AI = 80/20)	7600	2316.48

The fragment distribution factor, M_A is dependent upon the casing diameter and thickness of casing as is mentioned in Eqn. (7),

$$M_A = Bt_c^{\frac{5}{6}}d_i^{\frac{1}{3}}\left(1+\frac{t_c}{d_i}\right) \tag{7}$$

where, B is the explosive constant from Table 2, t_c is casing thickness and d_i is inside diameter of casing.

Table 2. Mott scaling constants for mild steel casings and various explosives[36]

Explosive	$Boz^{\frac{1}{2}\frac{-3}{2}}$	$Bkg^{\frac{1}{2}}m^{\frac{-3}{2}}$
Baratol	0.512	21.284
Composition A-3	0.220	9.145
Composition B	0.222	9.229
Cyclotol (75/25)	0.197	8.189
H-6	0.276	11.473
HBX-1	0.256	10.642
HBX-3	0.323	13.427
Pentolite (50/50)	0.248	10.309
PTX-1	0.222	9.229
PTX-2	0.227	9.436
RDX 0.205	0.212	8.813
Tetryl 0.265	0.272	11.307
TNT 0.302	0.312	12.970

The mass of fragments produced on detonation of cased explosive can be estimated by assuming several fragments as mentioned in Eqn. (8)

$$N_f = \frac{8W_c e^{-\left[\sqrt{\frac{W_f}{M_A}}\right]}}{M_A^2} \tag{8}$$

where, N_f is the number of fragments assumed (when the weight of each fragment is more significant than W_f), Wc is the casing weight as mentioned before, and W_f is the fragment weight assumed. The largest fragment would be when N_f =1. The weight of the largest fragment can be estimated using Eqn. (9)

$$W_c = \left[M_A \ln\left(\frac{8W_c}{M_A^2} \right) \right]^2 \quad (9)$$

The total number of fragments (N_T) can be predicted by considering $W_f = 0$ as expressed in Eqn. (10),

$$N_T = \frac{8W_c}{M_A^2} \quad (10)$$

The average fragment weight (W_f) is depicted in Eqn. (11),

$$W_f = \frac{16W_c}{N_T} = 2M_A^2 \quad (11)$$

The velocity of fragments is maximum when the source of the explosion is closer to the object (walls subjected to the explosion) and vice versa. The variation can also be influenced by the material properties of the casing[36]. The striking velocity on impact with the objects nearby can be determined as mentioned in Eqn. (12).

$$v_s = v_o e^{-[12k_v R_f]} \quad (12)$$

where, V_s is fragment speed at a distance R_f from the center of detonation, v_0 is the first (maximum) fragment speed, and k_v is velocity decay coefficient. The decay in the velocity of fragments occurs if the weight of the fragment is more; however, the code-based approach mentions the velocity decay coefficient k_v as mentioned in Eqn. (13),

$$k_v = \left(\frac{A}{W_f} \right) \rho_a C_D \quad (13)$$

where, A is the presented area of fragment, W_f is fragment weight, $\frac{A}{W_f}$ is fragment form factor, ρ_a is specific density of air and C_D is drag coefficient. The decay coefficient is evaluated as, $\frac{A}{W_f} = \frac{0.78}{W_f^{\frac{1}{3}}}$ for a random mild steel fragment, $\rho_a = 0.00071$ oz/in^3 (1.2283 kg/m^3) and $C_D = 0.6$ for primary fragments. Thus, striking velocity v_s now becomes as mentioned in Eqn. (14),

$$v_s = v_o e^{-\left[\frac{0.004 R_f}{W_f^{\frac{1}{3}}} \right]} \quad (14)$$

where, v_s is fragment velocity at a distance R_f from the centre of detonation, v_o is initial (maximum) fragment velocity and W_f is fragment weight.

3. ESTIMATION OF INITIAL AND STRIKING VELOCITY OF PRIMARY FRAGMENTS USING FINITE ELEMENT ANALYSIS

Potential damage to structures and humanity prior/post the artificial or accidental threat can be estimated with numerical analysis to minimize or prevent it. Herein, a numerical simulation study uses the 3D Finite Element tool LS DYNA. The explosive's steel box-type structure and casing are modeled in the Lagrangian domain with fully integrated shell elements. In contrast, the air is modeled using eight-node brick elements with Arbitrary Lagrangian-Eulerian (ALE) formulation. The explosives are modeled using the volume fraction method with the John-Wilkins-Lee (JWL) equation of state. Explosive is a volume coupled with air to transfer the shock wave through the air to the structure. The coupled interaction is considered between the Lagrangian and Eulerian parts. The study's objective is to perform fragment analysis using the Multi-Material Arbitrary Lagrangian and Eulerian (MMALE) approach. The output parameters estimated using the numerical simulations include primary fragments' initial and striking velocity. The detailed FE modeling procedure has been described in the following sections systematically.

3.1. Numerical Simulations for Material Models

3.1.1 Model for Steel

The non-linear elastic-plastic response is depicted using a material strength model. Unlike classic plasticity theory, this model reproduces significant critical responses of material seen in metal impact and penetration. For example, strain hardening, strain-rate effects, and heat softening are the three principal material reactions that predict the yield stress (σy) of material, as depicted in Eqn. (15).

$$\sigma_y\left(\varepsilon_p, \varepsilon_p^*, T\right) = \left(A + B\left(\varepsilon_p\right)^n ()\left(1 + C \ln \varepsilon_p^*\right)\left(1 - (T)^m\right)\right) \quad (15)$$

Here ε_p is equivalent plastic strain, ε_p^* is plastic strain rate, and A, B, C, n, m are material constants. Normalized strain rate and temperature of Eq. (13) are defined in Eqns. (16) and (17) respectively as,

$$\varepsilon_p^* = \frac{\varepsilon_p}{\varepsilon_{po}} \quad (16)$$

$$T^* = \frac{(T - T_0)}{(T_m - T_0)} \quad (17)$$

Here ε_p is a user specified plastic strain rate, ε_{po} is reference plastic strain. T_0 is reference temperature and T_m is reference melting temperature for conditions where $T^* < 0$, it is assumed that $m = 1$. The material properties and Johnson-Cook parameters used for modelling structural steel[37] are listed in Table 3 used to simulate material behaviour under a high rate of loading.

Table 3. Johnson-Cook model for steel[37]

Material	*A* (MPa)	*B* (MPa)	*C*	*n*
Steel	360	635	0.075	0.114

3.1.2 *Material Model for Explosive*

An explosion in the medium creates a mass of highly compressed gas that interacts with the surrounding medium to generate an outward propagating compressive shock front. The loading effect due to such an event can be defined as spherical incident waves for a conned air blast scenario using the JWL equation of state with the MMALE approach. The JWL equation of state describes the detonation product expansion down to a pressure of 1 k bar for high-energy explosive materials. It has been proposed by Jones, Wilkins, and Lee according to the following equation. Explosive is modeled using TNT equivalency according to the Jones-Wilkins-Lee equation of state as given by Eqn. (18)

$$p = A\left(1-\frac{w\eta}{R_1}\right)e^{\frac{-R_1}{\eta}} + B\left(1-\frac{w\eta}{R_2}\right)e^{\frac{-R_1}{\eta}} + w\rho e \qquad (18)$$

Here, ρ_0 is density of explosive in reference (in non-deformed state), ρ is current density of explosive on detonation and $\eta = \rho/\rho_0$. Values of the constants *A, B,* R_1, R_2 *and* ω for many general explosives have been experimentally determined. The properties of TNT used in the present work are given in Table 4.

Table 4. Material properties for TNT explosive[38]

Density (kg/m³)	A (kPa)	B (kPa)	R_1	R_2	W
1630	3.73×10^8	3.747×10^6	4.15	0.9	0.35

3.1.3 *Model for Air*

The air domain is formed using 3D Euler Multi-Material to fill the part with suitable geometry and boundaries to simulate the actual field scenario. Then, the air domain is generated using the linear polynomial equation of state (EoS) based on density and internal energy with other properties, as shown in Table 5. Finally, the air medium is assigned the ow-out boundary condition, best suited for modeling the explosive detonation.

Table 5. Properties of air at ambient conditions[38]

Density (g/cm³)	EoS	Gamma	Reference Temperature (K)	Specific Heat (J/mKs)
0.00122	Ideal gas	1.4	288.2	717.59

3.2 Structural Configuration

The box-type steel structure built from Q235 steel is modeled and subjected to an internal cased explosion to observe primary fragmentation. The steel box structure of 4 mm thick walls with a length of each side plate of 600 mm and an extra projection length of 120 mm is subjected to conned cased explosion[39]. The steel casing is spherical and used as an explosive shell. The varying explosives of 2 kg and 10 kg of TNT depict the initial and striking fragment velocities on detonation. The steel casing diameter depends upon the charge weight of the explosive. Herein, for the charge weight of 2 kg, the internal diameter of the casing is kept at 180 mm, and the outer diameter is considered 188 mm, wherein, for 10 kg explosive weight, the internal and outer diameter of the casing is 300 mm and 308 mm, respectively. The numerical investigation is carried out to predict the velocities of primary fragments generated from steel casing after an explosion inside the steel structure. The schematics of structure and explosive modeling are depicted in Fig. 2.

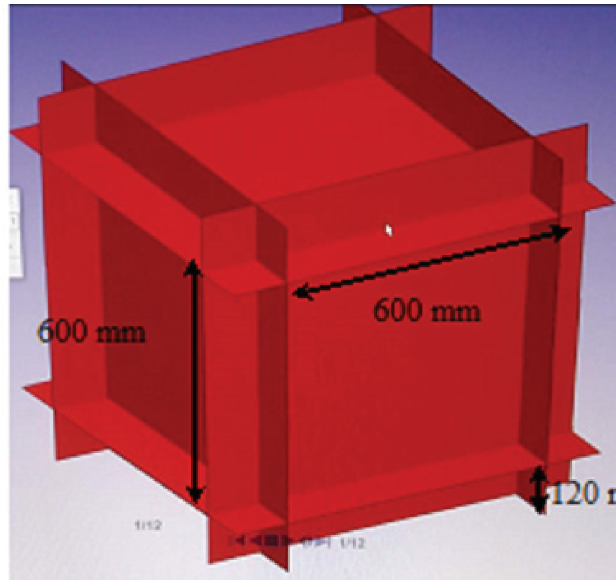

(a)

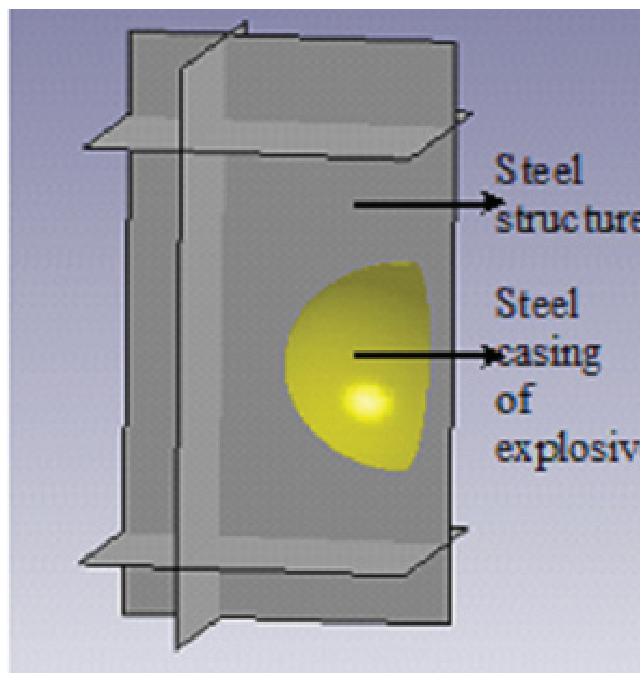

(b)

Figure 2. (a) Full numerical model for steel box type structure and (b) Quarter numerical model for steel box type structure with cased explosive.

The mesh convergence study is carried out to account for the computational efficiency of primary fragment velocity estimation. The fragment velocity of the primary fragments is estimated and plotted using different mesh sizes of 5 mm, 8 mm, 10 mm, 15 mm, 20 mm, and 30 mm for steel casing individually, as depicted in Fig. 3. Considering the total computational time and reasonable accuracy, a mesh size of 8 mm is chosen here for numerical analysis.

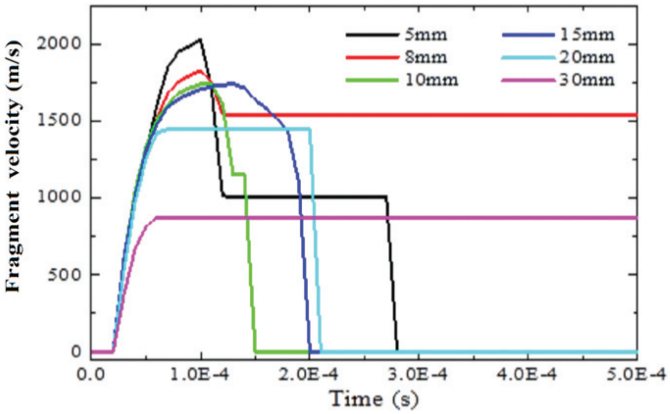

Figure 3. Mesh convergence study for estimation of primary fragment velocity.

4. RESULTS AND DISCUSSIONS

Numerical simulations have been carried out to predict the fragmentation phenomenon caused by an internal explosion. The cubical box-shaped steel structure has been subjected to internal explosion with a cased spherical explosive of TNT. The shock wave first interacts with the casing material, and fragmentation is observed. The casing material is of prime importance in fragment analysis as the capability of the casing to resist plastic strain will decrease the striking velocity and number of fragments. Herein, the steel-cased fragment velocity is studied. However, the fragmenting impact on the wall of the steel structure is not studied and can be kept for a further scope of work. The fragment impact on the walls of the steel structure on detonation of 2 kg of explosive is observed as depicted in Fig. 4. The behavior of steel structure on internal cased explosion is observed in terms of pressure generated on the inner wall of steel structure and effective plastic strain of steel structure.

Figure 5 and Figure 6 show pressure and strain contours experienced by the inner face of a cubical type steel structure with a charge weight of 2 kg TNT and 10 kg TNT bursting at the center of the structure. The steel structure remained elastic, while the explosive casing experienced high plastic strain, resulting in fragmentation. Moreover, these fragments move at a different initial and striking velocity, impacting the steel structure's inner face. Therefore, in case of an internal blast of cased explosive, apart from pressure and impulse, the fragmentation effects also need significant consideration.

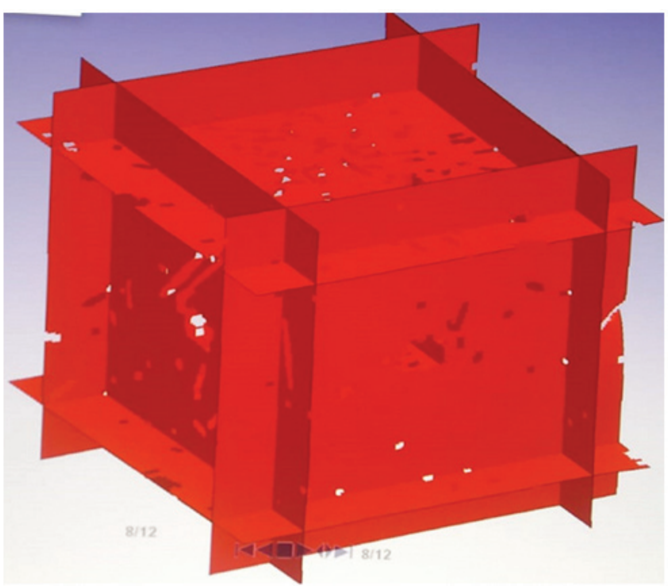

Figure 4. Fragment impact on walls of steel box structure on detonation of 2 kg explosive.

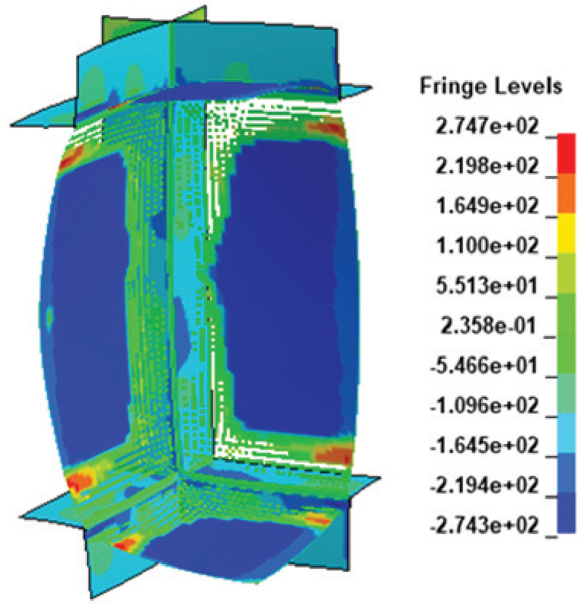

(a)

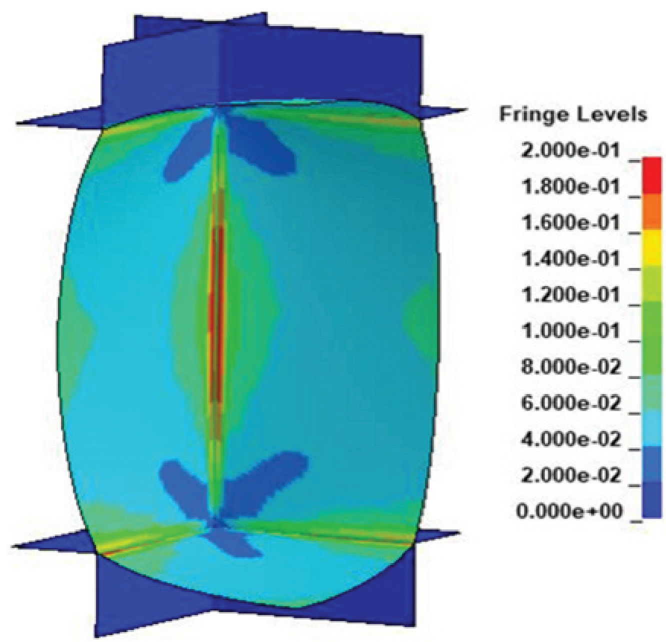

(b)

Figure 5. (a) Pressure contour in MPa for 2 kg explosion in 4 mm thick box type steel structure and (b) Effective plastic strain contour for 2 kg explosion in 4 mm thick box type steel structure.

Figure 7 shows the displaced position of the steel metal case due to internal explosion with varying charge weights, which signifies consideration of fragment effect while analyzing such a cubical structure. In addition, the sacrificial wall is also analyzed by reducing the thickness of the wall to observe the effect on fragment velocities.

It was observed that the velocity of fragments remains the same with and without a sacrificial wall for the same charge weight. Therefore, the trajectory of fragments can be controlled with the sacrificial wall, which is required to design preformed warheads.

The initial and striking velocities of primary fragments were estimated for varying charge weights, as depicted in the velocity time history plot in Figure 8. The initial and striking velocity for 2 kg explosive weight is almost the same. However, when the charge weight is increased to 10 kg, it is observed that striking velocity reduces to 1544 m/s from the initial velocity value of 1830 m/s, thereby establishing a correlation between

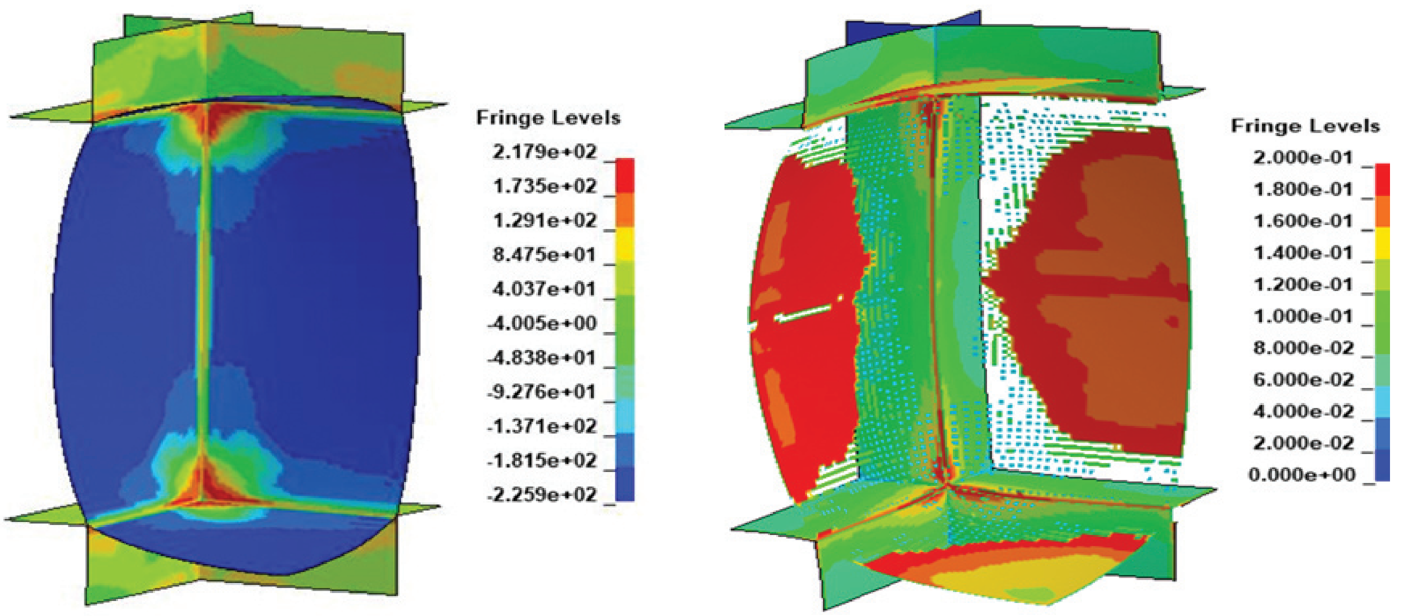

(a) **(b)**

Figure 6. (a) Pressure contour in MPa for10 kg explosion in 4 mm thick box type steel structure and (b) Effective plastic strain contour for 10 kg explosion in 4 mm thick box type steel structure.

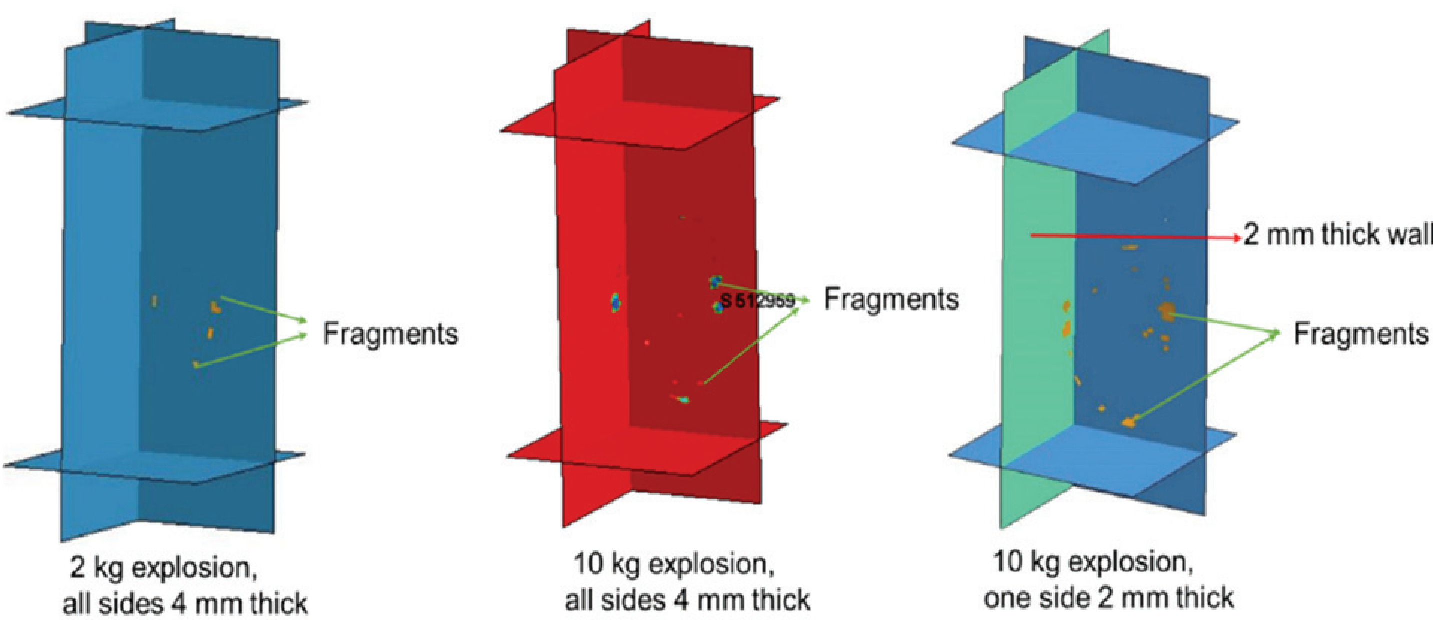

Figure 7. Position of fragments due to internal explosion with varying charge weights of 2 kg and 10 kg with thickness of 4 mm and sacrificial wall of thickness 2 mm of steel structure.

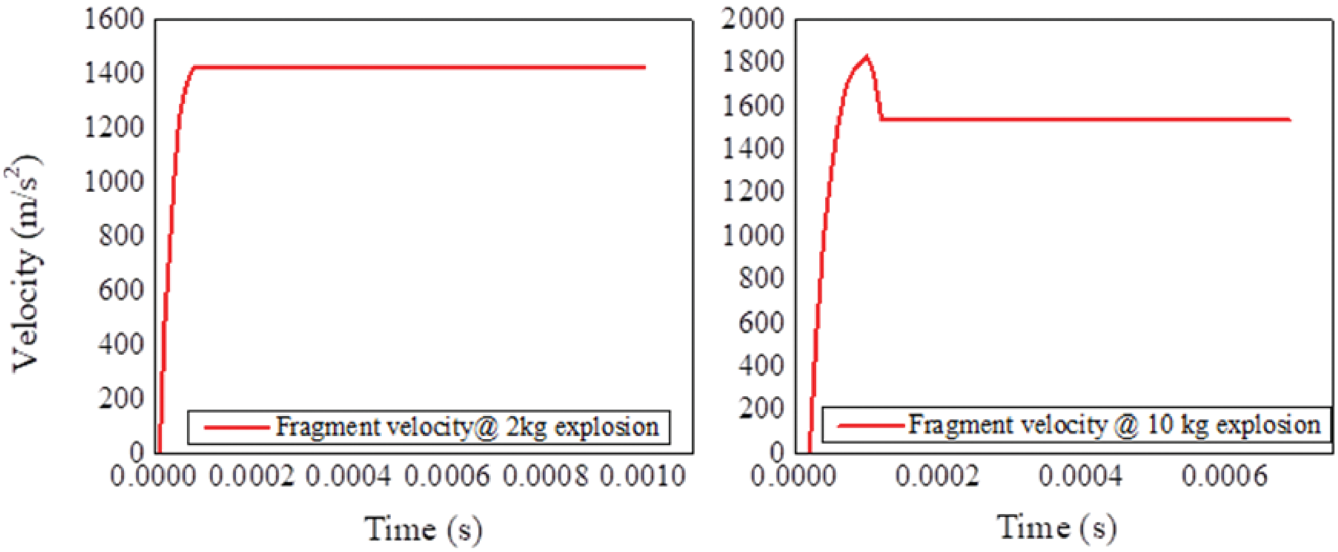

Figure 8. Velocity time history for initial velocity of primary fragments.

Table 6. Initial and striking velocity comparison for steel structure due to internal explosion of cased spherical explosive of weights of 2 kg and 10 kg.

Explosive weight	Velocity of primary fragments	Numerical simulation results from present study	Code based approach[36]	Percentage of difference (%)
2 kg	Initial velocity (m/s)	1337	1324	0.92
	Striking velocity (m/s)	1160	1222	5.3
10 kg	Initial velocity (m/s)	1830	1704	6.89
	Striking velocity (m/s)	1544	1524	1.28

the charge weight and the velocity of fragments. The numerical estimation of initial and striking velocities for 2 kg and 10 kg explosive weights were verified with a code-based approach via United Facilities Criteria (UFC-3-340, 2008) and found to be in good agreement, as expressed in Table 6. The casing material plays a vital role in primary fragment generation and estimation, ultimately responsible for the secondary fragments' impact on surrounding structures.

5. CONCLUSIONS

This paper investigates the fragmentation of spherical cased explosives enclosed in a steel cubicle box and explores a practical and convenient method to predict the initial and striking velocities of primary fragments. The simulation for an explosion of two charge weights of TNT was carried out, and the numerical results are validated through comparison with the UFC code approach. A good agreement is reported.

The numerical analysis confirms that fragment velocity and the difference in initial and striking velocity of fragments is a direct function of charge weight. Furthermore, one wall of cubical steel box was made a sacrificial wall by reducing the thickness to 2 mm, and fragmentation was observed. The results show that the sacrificial wall fails first, and controlled fragmentation is observed, which will help design preformed or directed fragmentation warheads.

ACKNOWLEDGEMENTS

The authors acknowledge support extended by Dr Vasant Matsagar, Civil Engineering Department, Indian Institute of Technology, Delhi during execution of this work.

REFERENCES

1. Taylor, G.I. Analysis of the explosion of a long cylindrical bomb detonated at one end. 1941.
2. Gurney, R.W. The initial velocities of fragments from bombs, shell and grenades. Aberdeen, MD, US: Ballistic Research Laboratory, 1943.
3. Hoggatt, C.R. and Recht R.F. Fracture behavior of tubular bombs. *J. Appl. Phy.*, 1968, **39**, 1856 – 1862.
4. Jones, G. E.The Gurney equations for multi layered fragments. *J. Appl. Phys.*, **50**, 3746–3747, 1979.
5. Jones, H. and Miller, A.R. The detonation of solid explosives. Proc. Roy. Soc. London, A-194, 480, 1948.
6. Wilkins, M.L.The equation of state of PBX 9404 and

LX04-01. Lawrence Radiation Laboratory, Livermore, report UCRL-7797, 1964.

7. Lee, E.L., Hornig, H.C. and Kury, J. Adiabatic expansion of high explosive detonation products. Univ. of California Radiation Lab: Livermore, CA, USA, 1968.
8. Charron, Y.J. Estimation of velocity distribution of fragmenting warheads using a modified gurney method. *Tech. rep.*, Air Force Institute of Technology, **113**, 1979.
9. Pearson, J. Fragmentation model for cylindrical warheads. Naval Weapons Center: China Lake, CA, USA, 1990.
10. Bola, M.S.; Madan, A.K. & Singh, M. Expansion of metallic cylinders under explosive loading. *Def. Sci. J.*, **42**, 157–163, 1992.
11. Kury, J.W.; Hornig, H.C.; Lee, E.L.; Mcdonnel, J.L.; Ornellas, D.L.; Finger, M.; Strange, F.M. & Wilkins, M.L. Metal acceleration by chemical explosives. Proceedings of the Fourth Internativnal Symposium on Detonation, Maryland, 12-15 October 1965, 1-13.
12. Cooper, P.W. Explos. Eng. Wiley-VCH, Chichester, New York, Weinheim, 1996.
13. Zukas, J.A. Explosive effects and applications. Springer-Verlag, Berlin, Heidelberg, New York, 1997.
14. Koch, A.; Arnold, N. & Estermann, M. A simple relation between the detonation velocity of an explosive and its Gurney energy. *Propellants, Explos., Pyrotech.*, 2002, **27**(6), 365-368.
15. Zhang, Qi. & Qing, M.C. Relation of fragment with air shockwave intensity for explosion in a shell. *Int. J. Impact Eng.*, 2003, **28**, 1129–1141.
16. Danel, J.F. and Kazandjian, L. A few remarks about the gurney energy of condensed explosives. *Propellants Explos. Pyrotech.*, 2004, **29**(5), 314–316.
17. Hutchinson, M.D. With-Fracture gurney model to estimate both fragment and blast impulses. *Central European J. Energetic Mater.*, 7.2, 175–186, 2010.
18. Breech, B.A. Extension of the gurney equations to two dimensions for a cylindrical charge. DTIC Document, 2011.
19. Felix, D.; Colwill, I. & Stipidis, E. Real-time calculation of fragment velocity for cylindrical warheads. *Def. Technol.*, 2019, **15**(3), 264-271.
20. Karpp, R.R. & Predebon, W.W. Calculations of fragment velocities from naturally fragmenting munitions. Ballistic Research Laboratories: Aberdeen, MD, USA, 1975.
21. Lindsay, C.M.; Butler, G.C.; Rumchik, C.G.; Schulze, B.; Gustafson, R. &SSSSS Maines, W.R. Increasing the utility of the copper cylinder expansion test. *Propellants Explos. Pyrotech.*, 2010, **35**, 433–439.
22. Breech, B.A. Extension of the gurney equations to two dimensions for a cylindrical charge. DTIC Document, 2011.
23. Elek, P.; Jaramaz, S. and Mickovic, D. Modeling of the metal cylinder acceleration under explosive loading. Scientific Technical Review, 2013, **63**(2), 39-46.
24. Wang, M.; Lu, F.; Li, X. and Cao, L. A formula for calculating the velocities of fragments from velocity enhanced warhead. *Propellants Explos. Pyrotech*., 2013, **38**, 232–237.
25. Xiangshao, K.; Wu, W. & Li, J. A numerical investigation on explosive fragmentation of metal casing using smoothed particle hydrodynamic method. *Mater. Des.*, 2013, **51**(60), 729-741.
26. Li, W.; Huang, G.Y. & Feng, S.S. Effect of eccentric initiation on the fragment velocity distribution of a cylindrical casing filled with charge. *Int. J. Impact Eng.*, 2010, **80**, 107–115.
27. Grisaro, H. & Dancygier, A.N. Numerical study of velocity distribution of fragments caused by explosion of a cylindrical cased charge. *Int. J. Impact Eng.*, 2015, **86**, 1-12,.
28. Gold, V.M. Fragmentation model for large l/d (length over diameter) explosive fragmentation warheads. *Def. Technol.*, 2017.
29. Huang, G.Y.; Li,W. & Feng, S.S. Axial distribution of Fragment Velocities from cylindrical casing under explosive loading. *Int. J. Impact Eng.*, 2015.
30. Li, Y.; Li, Y.H. & Wen, Y.Q. Radial distribution of fragment velocity of asymmetrically initiated warhead. International Journal of Impact Engineering, 2016, **99**, 39-47.
31. Wang, X.Y.; Wang, S.S. & Ma, F. Experimental study on the expansion of metal cylinders by detonation. *Int. J. Impact Eng.*, 2018, **114**, 147–152.
32. Felix, D.; Colwill, I. & Stipidis, E. Real-time calculation of fragment velocity for cylindrical warheads. *Def. Technol.*, 2019, **15**, 3, 264-271, .
33. Zhou, M.; Wu, C.; An, F.; Liao, S.; Yuan, X.; Xue, D. & Liu, J. Acceleration characteristics of discrete fragments generated from explosively-driven cylindrical metal shells. Mater., 2020, **13**(9), 2066.
34. An, X.; Dong, Y.; Liu, J. & Ye, P. Fragment velocity characteristics of warheads with a hollow core under asymmetrical Initiation. *Propellants Explos. Pyrotech.*, 2019, **44**, 1049–1058.
35. Jifeng, Wei; Zhixin, Du; Yonghui, Zheng; Liang, Zhang & Zhenbin, Lv. The fragmentation of thin-walled Q235 steel shell under explosion. IOP Conf. Series: *Mater. Sci. Eng.*, **768**(2020) 022033. doi:10.1088/1757-899X/768/2/022033.
36. Structures to Resist the Effects of Accidental Explosions (U.S. 2008), Unified Facilities Criteria UFC 3-340-02, US Department of the Army, 2008.
37. Matsagar, V.A. Comparative performance of composite sandwich panels and non-composite panels under blast loading. *Mater. Struct.*, 2016, **49**(1-2), 611 – 629.
38. Kloster, M.S. Coupled lagrangian and euleria approach to detonation and fragmentation problems. Master of Science Thesis, Naval Postgraduate School, Monetery, California, 2001.
39. Zhang, D.; Yao, S.; Lu, F.; Song, J. & Ding, Y. Dynamic response and damage analysis of steel box wall under internal blast loading. Advances in Mechanical Engineering, 2019.
40. LS-DYNA, Keyword user's manual, Material models, 2012, **2**(971), R6.1.0, Livermore Software Technology Corporation.

CONTRIBUTORS

Mr Prahlad Srinivas Joshi is an officer of Indian Air Force. He has rich and varied experience in the armament field and has served in various capacities in the formation including two tenures of being a chief engineering officer. The officer has vast knowledge in the field of aeronautics and maintenance of engineering assets involved in aviation. He is currently posted at Aeronautics Research and Development Board in DRDO HQ. He is a post graduate in Aerospace Engineering from Indian Institute of Science, Bengaluru and is a research scholar with DIAT, Pune.
His contribution to the current study − Literature survey, simulation trials, manuscript writing and validation of simulation

Dr S.K. Panigrahi obtained his PhD degree in Mechanical Engineering from the Indian Institute of Technology, Kharagpur, in 2007. He joined as Associate Professor at the Defence Institute of Advanced Technology (Deemed to be University), DRDO, Ministry of Defence, and GoI India in 2010. He was promoted to Professor in the year 2014. Presently he is heading the Department of Mechanical engineering for the second term and he is also a Director (Additional Charges) for the School of Robotics. Before joining the DIAT (DU). He has more than 28 years of comprehensive and intensive teaching, research, training, and administrative experience. His research works primarily in the areas of Analysis and Design of composite materials, Characterization of FRP composite materials, Finite Element Analysis of FRP composite materials and composite structures, Natural Fiber Reinforced Composite (NFRC) materials, Fracture Mechanics principle applicable to modelling and simulation of damages in orthotropic and isotropic materials and material characterization/ Stress analysis/Solid Mechanics/Machine design.
His contribution to the current study − Supervision, interpretation of simulation results and vetting of manuscript.